Available online at www.sciencedirect.com

SCIENCE DIRECT

Thin Solid Films 484 (2005) 251 – 256

thin solid films

www.elsevier.com/locate/tsf

Effects of residual stress on the thin-film elastic moduli calculated from surface acoustic wave spectroscopy experiments☆

R.E. Kumon*, D.C. Hurley

Materials Reliability Division, National Institute of Standards and Technology, 325 Broadway, Boulder, Colorado 80305-3328, USA

Received 9 December 2004; accepted 23 February 2005
Available online 26 April 2005

Abstract

We describe a method to examine how residual stress affects the values of thin-film elastic moduli determined from surface acoustic wave spectroscopy experiments. To illustrate our approach, we apply it to the case of an elastically isotropic thin film under equibiaxial stress. The five test samples consisted of TiN films deposited on single-crystal Si substrate (film thickness 0.287–3.330 μm and assumed compressive stress 0.5–5.4 GPa). With increasing thickness and decreasing stress, the effective second-order moduli C_{11} increased and C_{13} decreased. The natural second-order elastic moduli c_{11} and c_{13} and the natural third-order elastic moduli c_{111}, c_{112}, and c_{123} in the unstressed state were computed by fitting the model equations to the measured data. Our results show how surface acoustic wave measurements may be analyzed to obtain additional information about the mechanical properties of thin films with residual stress.
Published by Elsevier B.V.

PACS: 68.60.Bs; 62.20.Dc; 62.65.+k; 43.35.Ns
Keywords: Acoustoelastic effect; Elastic properties; Residual stress; Surface acoustic waves; Titanium nitride

1. Introduction

Thin supported films can have significant residual stresses, sometimes as large as several gigapascals [1]. These stresses typically arise due to the mismatch between the thermal expansion coefficients or lattice constants of the film and substrate [2]. Such stresses change the film's physical properties, thereby affecting its eventual performance or lifetime in manufactured products. Current experimental techniques for measuring stress in thin films can be basically divided into two broad categories: lattice strain methods, including X-ray and neutron diffraction, and physical surface curvature-based methods, including double crystal diffraction topography, profilometry, laser scanning techniques, and optical interferometry. Each of these techniques has its own limitations. For example, lattice strain methods are limited to crystalline materials, laser scanning techniques are less effective for surfaces with low reflectivity or high roughness, and profilometry is typically destructive [3]. In this paper, we describe our efforts to develop an alternative, complementary method based on surface acoustic wave methods.

Surface acoustic wave (SAW) spectroscopy has been established as a non-contact, nondestructive technique for measuring the elastic properties of thin films [4]. SAWs are well suited to this task because their energy is naturally concentrated near the surface and in the thin film. Furthermore, SAWs are affected by residual stress. This is because the SAW velocity is determined by the second-order elastic moduli and density of the film and substrate materials, and both the elastic moduli and density are changed by the stress. The exact relationship is generally very complicated, and typically a numerical solution of the model equations is required. This so-called

☆ Contribution of NIST, an agency of the US government; not subject to copyright.

* Corresponding author. Current address: Department of Physics, University of Windsor, 401 Sunset Ave., Windsor, Canada, ON N9B 3P4.
E-mail address: ronkumon@kumonweb.com (R.E. Kumon).
URL: http://www.kumonweb.com/ron/pro/ (R.E. Kumon).

0040-6090/$ - see front matter. Published by Elsevier B.V.
doi:10.1016/j.tsf.2005.02.033

acoustoelastic effect is typically very small (only a fraction of a percent change in velocity), but has been successfully used to measure the residual stress in bulk materials [5,6].

Acoustic determination of stress in thin-film systems may also be possible, due to the combination of the high precision of SAW measurements and the high values of residual stress that can occur. Theoretical models have been developed to describe the effect of stress on Love, Rayleigh-type, and Sezawa modes [7,8]. In addition, agreement has been obtained between theory and experiment for the SAW dispersion of stressed silver films on a crystalline silicon substrate [9]. As these papers demonstrate, the effects of stress on the thin film can be computed in terms of "effective" (stressed) second-order elastic moduli and density if the second- and third-order elastic moduli and density are known in the "natural" (unstressed) state [10]. Unfortunately, for many new materials these moduli may not be known for either the film or the bulk state.

To address this problem, we present a method for computing the natural second- and third-order elastic moduli of a material from values of the effective second-order elastic moduli measured from thin-film samples in several known stressed states. It may then be possible to use these natural moduli to acoustically determine the residual stress in samples with unknown stress. To illustrate our approach, we present results for a series of TiN films deposited on a monocrystalline Si substrate. The films are assumed to be elastically isotropic and to have equibiaxial residual stress. Although the results presented here apply to a specific set of samples, the methods we describe are sufficiently general to be adapted to a wide range of thin-film systems comprised of different film materials, thicknesses, and stress states.

2. Theory

Consider a system consisting of a single layer on a half-space, as shown in Fig. 1. Let the Cartesian coordinates of a particle in the *natural* (unstressed) state be denoted by a, in the *initial* (pre-stressed) state by X_i, and in the *current* (acoustic) state by x_i [5].

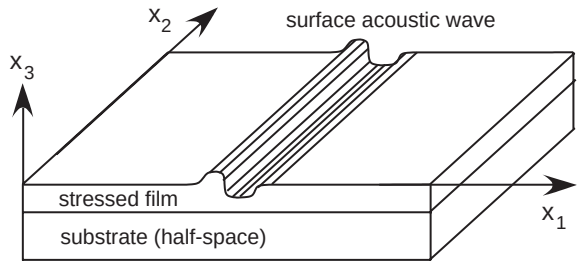

Fig. 1. Schematic diagram of thin-film system with coordinate axes.

2.1. Initial (pre-stressed) state of orthotropic film

Assume that a Cauchy pre-stress σ_{ij}^0 exists in the layer, but not the substrate. Also assume that the infinitesimal pre-strain e_{ij}^0 is related to the pre-stress by

$$\sigma_{ij}^0 = c_{ijkl} e_{kl}^0, \tag{1}$$

where c_{ijkl} are the natural second-order elastic moduli,

$$e_{ij}^0 = \frac{1}{2}\left(\frac{\partial U_i^0}{\partial a_j} + \frac{\partial U_j^0}{\partial a_i}\right) \tag{2}$$

is the infinitesimal strain tensor, and

$$U_i^0 = X_i - a_i \tag{3}$$

is the displacement of the initial coordinates relative to the natural coordinates. If the lateral pre-stress σ_{ij}^0 in the layer is biaxial and equal in both directions, then it follows that [7]

$$\sigma_{11}^0 = \sigma_{22}^0 = \sigma, \quad \sigma_{33}^0 = \sigma_{12}^0 = \sigma_{23}^0 = \sigma_{13}^0 = 0, \tag{4}$$

where the coordinate axes are chosen such that the x_3 axis is normal to the surface of the film (Fig. 1). Finally assume that the medium under study has at least orthotropic symmetry with the nine independent elastic moduli: c_{11}, c_{12}, c_{13}, c_{22}, c_{23}, c_{33}, c_{44}, c_{55}, c_{66}. Reduced-index Voigt notation [11] is used for elastic moduli throughout this paper except for equations where the repeated index (Einstein) notation is employed. Solving Eq. (1) for the pre-strains yields

$$e_{11}^0 = \frac{M_{22} - M_{12}}{M_{11}M_{22} - M_{12}^2}\sigma,$$

$$e_{22}^0 = \frac{M_{11} - M_{12}}{M_{11}M_{22} - M_{12}^2}\sigma,$$

$$e_{33}^0 = -\frac{c_{13}}{c_{33}}e_{11}^0 - \frac{c_{23}}{c_{33}}e_{22}^0, \tag{5}$$

where $M_{11} = c_{11} - c_{13}^2/c_{33}$, $M_{12} = c_{12} - c_{13}c_{23}/c_{33}$, and $M_{22} = c_{22} - c_{23}^2/c_{33}$. All other pre-strain components are zero under these assumptions.

2.2. Current (acoustic) state of orthotropic film

The effective elastic moduli C_{ijkl} evaluated in the current state relative to the initial state are [10]

$$C_{ijkl} = c_{ijkl}\left(1 - e_{mm}^0\right) + c_{ijklmn}e_{mn}^0 + c_{mjkl}\frac{\partial U_i^0}{\partial x_m} + c_{imkl}\frac{\partial U_j^0}{\partial x_m} + c_{jiml}\frac{\partial U_k^0}{\partial x_m} + c_{ijkm}\frac{\partial U_l^0}{\partial x_m}, \tag{6}$$

where c_{ijkl} and c_{ijklmn} are the natural second- and third-order elastic moduli. (We have assumed that the acoustic wave displacement is infinitesimal in nature so that the laboratory

frame is essentially the initial frame.) In the case of only axial stresses, Eq. (6) reduces to [7]

$$C_{ijkl} = c_{ijkl}\left(1 - e^0_{11} - e^0_{22} - e^0_{33} + e^0_{ii} + e^0_{jj} + e^0_{kk} + e^0_{ll}\right) + c_{ijkl11}e^0_{11} + c_{ijkl22}e^0_{22} + c_{ijkl33}e^0_{33}, \tag{7}$$

where there is no sum over repeated indices. In general, orthotropic media have twenty independent third-order elastic moduli: c_{111}, c_{112}, c_{113}, c_{122}, c_{123}, c_{133}, c_{144}, c_{155}, c_{166}, c_{222}, c_{223}, c_{233}, c_{244}, c_{255}, c_{266}, c_{333}, c_{344}, c_{355}, c_{366}, c_{456}. If the effective second-order elastic moduli and the natural third-order elastic moduli are known, then Eq. (7) are a system of nine equations with nine unknowns (c_{ijkl}) that can be easily solved given the pre-strains. However, often none or only a few of the natural third-order elastic moduli have been determined for materials of practical interest. (In some cases, not even all the effective second-order elastic moduli are known.) Hence the question remains as to what useful information can be extracted from Eq. (7) given these kinds of realistic constraints.

For ease of notation, let $e^0_{ii} = e_i$ (no sum over repeated indices) and $e = e_1 + e_2 + e_3$. Eq. (7) can be written out explicitly as

$$\begin{aligned}
C_{11} &= c_{11}(1 - e + 4e_1) + c_{111}e_1 + c_{112}e_2 + c_{113}e_3,\\
C_{22} &= c_{22}(1 - e + 4e_2) + c_{122}e_1 + c_{222}e_2 + c_{223}e_3,\\
C_{33} &= c_{33}(1 - e + 4e_3) + c_{133}e_1 + c_{233}e_2 + c_{333}e_3,\\
C_{23} &= c_{23}(1 - e + 2e_2 + 2e_3) + c_{123}e_1 + c_{223}e_2 + c_{233}e_3,\\
C_{13} &= c_{13}(1 - e + 2e_1 + 2e_3) + c_{113}e_1 + c_{123}e_2 + c_{133}e_3,\\
C_{12} &= c_{12}(1 - e + 2e_1 + 2e_2) + c_{112}e_1 + c_{122}e_2 + c_{123}e_3,\\
C_{44} &= c_{44}(1 - e + 2e_2 + 2e_3) + c_{144}e_1 + c_{244}e_2 + c_{344}e_3,\\
C_{55} &= c_{55}(1 - e + 2e_1 + 2e_3) + c_{155}e_1 + c_{255}e_2 + c_{355}e_3,\\
C_{66} &= c_{66}(1 - e + 2e_1 + 2e_2) + c_{166}e_1 + c_{266}e_2 + c_{366}e_3.
\end{aligned} \tag{8}$$

Nineteen of the twenty third-order elastic moduli appear in Eq. (8).

2.3. Current (acoustic) state of isotropic film

Consider the limiting case of an isotropic material placed under an equibiaxial stress. Isotropic materials have only two independent second-order elastic moduli [12]: $c_{11}=c_{22}=c_{33}$ and $c_{12}=c_{13}=c_{23}$, with the additional dependent relations $c_{44}=c_{55}=c_{66}=(c_{11}-c_{12})/2$. There are three independent third-order elastic moduli [13]: $c_{111}=c_{222}=c_{333}$, $c_{112}=c_{113}=c_{122}=c_{133}=c_{223}=c_{233}$, c_{123}, with the additional dependent relations $c_{144}=c_{255}=c_{366}=(c_{112}-c_{123})/2$, $c_{155}=c_{166}=c_{244}=c_{266}=c_{344}=c_{355}=(c_{111}-c_{112})/4$, $c_{456}=(c_{111}-3c_{112}+2c_{123})/8$. With these conditions, Eq. (8) reduce to

$$C_{11} = c_{11}(1 + 2e_1 - e_3) + (c_{111} + c_{112})e_1 + c_{112}e_3, \tag{9a}$$

$$C_{33} = c_{11}(1 + 2e_1 - e_3) + 2c_{112}e_1 + c_{111}e_3, \tag{9b}$$

$$C_{13} = c_{12}(1 + e_3) + (c_{112} + c_{123})e_1 + c_{112}e_3, \tag{9c}$$

$$C_{12} = c_{12}(1 + e_3) + 2c_{112}e_1 + c_{123}e_3, \tag{9d}$$

$$C_{44} = c_{44}(1 + e_3) + (c_{144} + c_{155})e_1 + c_{155}e_3, \tag{9e}$$

where $C_{22}=C_{11}$, $C_{23}=C_{13}$, $C_{55}=C_{44}$, and $C_{66}=(C_{11}-C_{12})/2$. These elastic constant relations correspond to a material with hexagonal symmetry [12]. Thus, deformation of an isotropic material by an in-plane equibiaxial stress results in a material with hexagonal symmetry properties.

2.4. Inversion method

Now we show how the relationships given above can be used to obtain thin-film mechanical property information. Suppose that the effective elastic moduli are known in $\alpha = 1, \ldots, N$ samples of different pre-stresses $\sigma^{[\alpha]}$ and pre-strains $e_i^{[\alpha]}$ with $e^{[\alpha]} = e_1^{[\alpha]} + e_2^{[\alpha]} + e_3^{[\alpha]}$ (the superscript 0 is dropped here for notational simplicity). Assume that the elastic moduli in each sample are the same in the unstressed state. Let the effective second-order elastic moduli in Voigt notation be given by $C_{IJ}^{[\alpha]} = C_{IJ}(\sigma^{[\alpha]})$ for each sample. Then for each sample, Eq. (7) implies that

$$C^{[\alpha]}_{ijkl} = c_{ijkl}\left(1 - e^{[\alpha]}_{11} - e^{[\alpha]}_{22} - e^{[\alpha]}_{33} + e^{[\alpha]}_{ii} + e^{[\alpha]}_{jj} + e^{[\alpha]}_{kk} + e^{[\alpha]}_{ll}\right) + c_{ijkl11}e^{[\alpha]}_{11} + c_{ijkl22}e^{[\alpha]}_{22} + c_{ijkl33}e^{[\alpha]}_{33}. \tag{10}$$

If enough samples are available with at least a few measured values of $C^{[\alpha]}_{ijkl}$ available for each, then it may be possible to solve for the values of the natural moduli c_{ijkl} and c_{ijklmn}.

For a film that is isotropic in its natural state, there are five unknown elastic moduli: c_{11}, c_{12}, c_{111}, c_{112}, and c_{123}. Suppose that the effective elastic moduli C_{11} and C_{13} are measured for a set of samples (e.g., see Section 3). The known effective moduli in each sample are related to the unknown natural moduli by Eq. (10), simplified in the form of Eq. (9a) and (9c):

$$C^{[\alpha]}_{11} = c_{11}\left(1 + 2e^{[\alpha]}_1 - e^{[\alpha]}_3\right) + (c_{111} + c_{112})e^{[\alpha]}_1 + c_{112}e^{[\alpha]}_3, \tag{11a}$$

$$C_{13}^{[\alpha]} = c_{12}\left(1 + e_3^{[\alpha]}\right) + (c_{112} + c_{123})e_1^{[\alpha]} + c_{112}e_3^{[\alpha]}. \quad (11b)$$

Eqs. (11a) and (11b) can be written out explicitly in matrix form as

$$\begin{pmatrix} C_{11}^{[1]} \\ C_{11}^{[2]} \\ C_{11}^{[3]} \\ C_{11}^{[4]} \\ C_{11}^{[5]} \\ C_{13}^{[1]} \\ C_{13}^{[2]} \\ C_{13}^{[3]} \\ C_{13}^{[4]} \\ C_{13}^{[5]} \end{pmatrix} = \begin{pmatrix} 1+2e_1^{[1]}-e_3^{[1]} & 0 & e_1^{[1]} & e_1^{[1]}+e_3^{[1]} & 0 \\ 1+2e_1^{[2]}-e_3^{[2]} & 0 & e_1^{[2]} & e_1^{[2]}+e_3^{[2]} & 0 \\ 1+2e_1^{[3]}-e_3^{[3]} & 0 & e_1^{[3]} & e_1^{[3]}+e_3^{[3]} & 0 \\ 1+2e_1^{[4]}-e_3^{[4]} & 0 & e_1^{[4]} & e_1^{[4]}+e_3^{[4]} & 0 \\ 1+2e_1^{[5]}-e_3^{[5]} & 0 & e_1^{[5]} & e_1^{[5]}+e_3^{[5]} & 0 \\ 0 & 1+e_3^{[1]} & 0 & e_1^{[1]}+e_3^{[1]} & e_1^{[1]} \\ 0 & 1+e_3^{[2]} & 0 & e_1^{[2]}+e_3^{[2]} & e_1^{[2]} \\ 0 & 1+e_3^{[3]} & 0 & e_1^{[3]}+e_3^{[3]} & e_1^{[3]} \\ 0 & 1+e_3^{[4]} & 0 & e_1^{[4]}+e_3^{[4]} & e_1^{[4]} \\ 0 & 1+e_3^{[5]} & 0 & e_1^{[5]}+e_3^{[5]} & e_1^{[5]} \end{pmatrix} \begin{pmatrix} c_{11} \\ c_{12} \\ c_{111} \\ c_{112} \\ c_{123} \end{pmatrix}, \quad (12)$$

or more compactly as

$$\mathbf{C} = \mathbf{E}\mathbf{c}. \quad (13)$$

Eq. (13) has the formal solution

$$\mathbf{c} = \mathbf{E}^{-1}\mathbf{C}, \quad (14)$$

provided that det $\mathbf{E} \neq 0$ (nonsingular). $\mathbf{E}$ may be singular because the values of $C_{11}^{[\alpha]}$ and $C_{13}^{[\alpha]}$ are not exactly known or because there are not enough values of $C_{11}^{[\alpha]}$ and $C_{13}^{[\alpha]}$ to fully determine the solution. Even if $\mathbf{E}$ is singular, it is still possible to obtain an approximate solution in a least-squares sense. It is always possible to decompose $\mathbf{E}$ via a singular-value decomposition [14] into the form

$$\mathbf{E} = \mathbf{U}\mathbf{W}\mathbf{V}^{\mathrm{T}}, \quad (15)$$

where $\mathbf{U}$ is a column-orthonormal matrix, $\mathbf{W}$ is a diagonal matrix with positive or zero elements, and $\mathbf{V}$ is a row-orthonormal matrix [14]. When $\mathbf{E}$ is singular, at least one of the diagonal elements w_i of $\mathbf{W}$ is zero. However, in these cases it possible to show that [14]

$$\mathbf{c} = \mathbf{V}\left[diag\left(w_j'\right)\right]\mathbf{U}^{\mathrm{T}}\mathbf{C} \quad (16)$$

is the solution that minimizes $|\mathbf{C} - \mathbf{E}\mathbf{c}|$, where

$$w_j' = \begin{cases} 1/w_j & \text{if } w_j \neq 0 \\ 0 & \text{if } w_j = 0 \end{cases}. \quad (17)$$

This latter technique may also be used if the system is overdetermined. The next section shows how this procedure can be followed in practice for an actual set of data.

3. Application to titanium nitride films

To illustrate the method described above, we apply it to SAW spectroscopy data for titanium nitride films on single-crystalline silicon substrates reported by Hurley, Tewary, and Richards [15]. In their experiments, they generated and detected broadband SAWs by laser-ultrasonic methods. Using Fourier transform techniques, they calculated the SAW phase velocity as a function of frequency (dispersion relation) for each sample. Because higher-frequency SAWs penetrate less deeply into the film–substrate system than do lower frequency SAWs, the properties of the film affect the former more strongly than the latter. Hence the various frequency components of the SAW pulses have different phase velocities. By comparing the measured dispersion relations to those predicted by an analytical model [16], they determined values for the film elastic moduli for five samples with increasing residual stress σ and thickness d. The properties of each sample are given in Table 1. The compressive residual stress for each film was determined by wafer bending methods. Under the assumption that the film had hexagonal symmetry, they computed only the effective elastic moduli C_{11} and C_{13}. Values for the other second-order elastic moduli (C_{12}=117 GPa, C_{33}=469 GPa, C_{44}=182 GPa) were taken as needed from the texture-averaged values calculated by Pang et al. [17] based on the single-crystal values from Perry [18].

To compute the pre-strains from the pre-stresses using Eq. (5), it is necessary to know the values of the elastic moduli c_{11} and c_{12}. This situation is problematic because these second-order elastic moduli are some of the quantities that are being sought. To resolve this issue, we assumed as initial guesses the calculated values (c_{11}=473 GPa, c_{12}=117 GPa) given by Pang et al. [17]. When we substituted the data from Table 1 into Eq. (13), we found that $\mathbf{E}$ is singular. Therefore we applied the least-squares solution of Eq. (16) to obtain values for the natural elastic moduli. Once the inversion of Eq. (16) was performed, we substituted these new values of the natural elastic moduli c_{ij} back into Eq. (5) and iterated this procedure a few times until the computed values converged. We found that the final solution was not very sensitive to the choice of the initial guess.

Our final results are shown in Table 2. The second-order elastic constants are in line with values reported in the literature for cubic symmetry [17,19–21]. Note that the third-order elastic moduli are not unique, as discussed below. We determined the uncertainties for the natural

Table 1
Comparison of measured and computed effective elastic moduli for TiN films on crystalline Si

Sample no.	σ (GPa)	d_{SAW} (nm)	C_{11}^{meas} (GPa)	C_{11}^{comp} (GPa)	C_{13}^{meas} (GPa)	C_{13}^{comp} (GPa)
5	0.5	3721±139	510±2	500	92±1	91
4	1.8	951±70	479±7	487	121±6	115
3	2.9	803±17	468±10	475	121±16	136
2	3.5	331±31	467±20	469	154±17	147
1	5.4	279±24	456±2	449	183±8	182

The measured residual stresses σ, effective elastic moduli C_{11}^{meas}, C_{13}^{meas}, and film thicknesses d_{SAW} are taken from Ref. [15]. The samples are ordered in the table with increasing stress but the sampling numbering has been retained from the original paper for consistency. The computed effective moduli C_{11}^{comp}, C_{13}^{comp} are derived by substituting the natural elastic moduli c_{ij} in Table 2 and residual stresses σ into Eqs. (5) (9a) – (9e) for the TiN film.

moduli by solving Eq. (13) two additional times using the upper and lower bounds of the measured effective moduli as shown in Table 1. In other words, we used all the maximum values of the measured effective moduli ($C_{11}^{meas}+\Delta C_{11}^{meas}$, $C_{13}^{meas}+\Delta C_{13}^{meas}$) in the first case, and used all the minimum values ($C_{11}^{meas}-\Delta C_{11}^{meas}$, $C_{13}^{meas}-\Delta C_{13}^{meas}$) in the second case to provide the estimates for the bounds for the natural moduli.

Once we had determined the natural elastic moduli, we then used these values and the residual stresses to evaluate Eqs. (5) (9a)–(9e) for the expected effective moduli C_{11}^{comp} and C_{13}^{comp}. Table 1 shows the quality of the fit for the effective moduli at each stress level obtained with the natural moduli in Table 2. The agreement is excellent (within the measured uncertainty) for all the values of $C_{13}^{comp}$and all except two of the values of C_{11}^{comp}. For those two values, the agreement is very good, with differences of less than 2%. In addition, the value for the natural c_{11} is larger than any of the effective C_{11}^{meas}, which is consistent with the trend for C_{11} to decrease with increasing residual stress. Likewise, the value for the natural c_{13} is smaller than any of the effective C_{13}^{meas}, which is consistent with the trend for C_{13} to increase with increasing residual stress.

Fig. 2 shows the measured effective elastic moduli of Table 1 along with the dependence of all the effective elastic moduli on the residual stress as predicted by Eq. (9a)–(9e). Observe that as $\sigma \rightarrow 0$, the values of the effective C_{11} and C_{33}, C_{12} and C_{13}, and C_{44} and C_{66} converge, as required for an elastically isotropic material. The shaded regions around each line in Fig. 2 indicate the estimated error for each calculated line based on the experimental uncertainties. Note that C_{44} and C_{66} are much less sensitive to the experimental uncertainty in C_{11} and C_{13}. In fact, the shaded regions are almost too small to see.

It should be mentioned that the least squares solution given by Eq. (16) for the third-order elastic moduli of Table 2 is not unique. Mathematically, the rank of the matrix **E** is less than five and hence its nullspace has dimension one. The reason for the lack of uniqueness is not entirely clear. It is possible that it is caused by the relatively small number of samples. The issue of uniqueness in the results of surface-acoustic-wave inversion methods is discussed in more detail in Ref. [22].

As this application shows, the model presented is useful in cases where predictions of the second-elastic moduli of a film are desired but third-order elastic moduli for the unstressed

Table 2
Natural elastic moduli computed from Eq. (13) for TiN film

Elastic modulus	Value (GPa)
c_{11}	505±7
c_{12}	82±5
c_{111}	5980±10
c_{112}	−2000±500
c_{123}	−9000±700

The third-order elastic moduli are not unique.

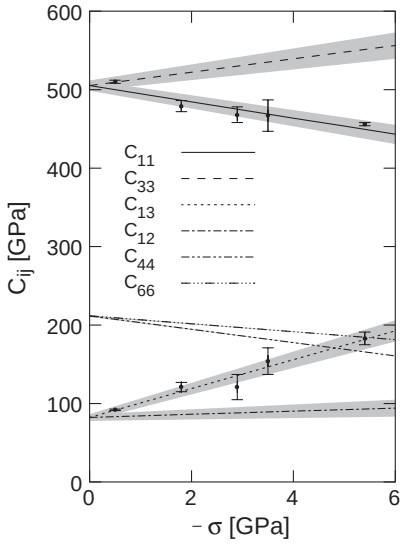

Fig. 2. Effective second-order elastic moduli C_{ij} as a function of the compressive stress σ. The lines show the values computed based upon Eqs. (5) (9b) – (9e), and the natural second-order moduli in Table 2, while the measured data from Ref. [15] in Table 1 are shown by the solid circles. The natural moduli c_{ij} occur at zero residual stress. For each elastic modulus, the shaded band around each line indicates the estimated error, computed from the experimental uncertainties for the effective moduli in Table 1.

state are unavailable. It is important to be aware of possible limitations of the approach based on its assumptions. First, the films are assumed to have a homogeneous equibiaxial stress state [Eq. (4)]. Based on previous studies, this assumption appears to be a good approximation in TiN films [23,24] and has also been used in other cases to perform calculations of the acoustoelastic effect in Ge films on Si [7,8,25]. Second, the films in this data set have different thicknesses in addition to different residual stresses, and this may have an effect on the film properties. For example, the films may have a stress gradient that changes with thickness. Finally, the plastic deformation that causes the residual stresses may cause other changes to the films that are not accounted for. We did not have a way to independently determine the magnitude of these effects for the TiN films.

The method outlined above involves several assumptions and thus may not be appropriate for some systems. Nonetheless, it should be useful for systems with simple initial stress distributions, film structure, and crystalline symmetries. It may also be possible to use in conjunction with systems where appropriate stresses may be applied to make the equibiaxial stress assumption hold. For the given case, this approach fits the data well and predicts the behavior of the elastic moduli that were not measured.

4. Summary and conclusions

We have presented a general method for determining the natural second-order elastic moduli c_{ijkl} and third-order

elastic moduli c_{ijklmn} of a thin film deposited on a substrate given the residual stress σ and effective second-order moduli C_{ijkl} in the film. We applied this method to the case of an elastically isotropic, biaxially-stressed TiN film deposited on a crystalline Si substrate. The effective second-order elastic moduli were taken from data previously determined from surface acoustic wave spectroscopy. To begin, an initial guess for the pre-strains in the film was determined from the measured residual stress and literature values for the second-order effective elastic moduli. Next, Eqs. (5) and (16) were solved iteratively until the solutions converged. To compute the quality of fit with the measured data, the theoretical effective elastic constants C_{ijkl} were then calculated from Eqs. (5) (9a)–(9e) using the previously computed natural elastic constants c_{ijkl} and c_{ijklmn}. The results in Fig. 2 showed that the method can fit the data well. With decreasing thickness and increasing stress, the effective second-order moduli C_{11}, C_{44}, and C_{66} decreased, while C_{13}, C_{33}, and C_{12} increased.

As described and implemented here, this method has some limitations. Additional theoretical and experimental work is needed to further develop the basic method presented. Nonetheless, we have demonstrated that by using this approach, it is possible to evaluate the natural second- and third-order elastic moduli from the effective second-order elastic moduli measured using an acoustical technique for a series of films in different residual stress states.

Acknowledgments

This research was performed while R.E.K. held a National Research Council Research Associateship Award at the National Institute of Standards and Technology.

References

[1] M. Ohring, The Materials Science of Thin Films, Academic Press, New York, 1992.
[2] W.D. Nix, Metall. Trans., A, Phys. Metall. Mater. Sci. 20A (1989) 2217.
[3] Z.B. Zhao, J. Hershberger, S.M. Yalisove, J.C. Bilello, Mater. Res. Soc. Symp. Proc. 505 (1998) 519.
[4] P. Hess, Phys. Today 55 (3) (2002) 42.
[5] Y.-H. Pao, W. Sachse, H. Fukuoka, in: W.P. Mason, R.N. Thurston (Eds.), Phys. Acoust., vol. 17, Academic Press, New York, 1984, p. 61.
[6] K.Y. Kim, W. Sachse, in: M. Levy, H. Bass, R. Stern (Eds.), Handbook of Elastic Properties of Solids, Liquids, and Gases, Vol. I: Dynamic Methods for Measuring the Elastic Properties of Solids, Academic Press, New York, 2001, p. 441, (Ch. 19).
[7] A.V. Osetrov, H.J. Frohlich, R. Koch, Phys. Rev., B 62 (2000) 13963.
[8] E. Chilla, A.V. Osetrov, R. Koch, Phys. Rev., B 63 (2001) 113308.
[9] A. Njeh, T. Wieder, D. Schneider, H. Fuess, M.H. Ben Ghozlen, Z. Naturforsch. 57a (2002) 58.
[10] Y.-H. Pao, U. Gamer, J. Acoust. Soc. Am. 77 (1985) 806.
[11] B.A. Auld, Acoustic Fields and Waves in Solids, 1st ed., vol. I and II, John Wiley and Sons, New York, 1973.
[12] R.F.S. Hearmon, in: K.-H. Hellwege, A.M. Hellwege (Eds.), Elastic, Piezoelectric, Pyroelectric, Piezooptic, Electrooptic Constants, and Nonlinear Dielectric Susceptibilities of Crystals, Vol. III/11 of Landolt-Bornstein, New Series, Springer-Verlag, New York, 1979, p. 1.
[13] R.F.S. Hearmon, in: K.-H. Hellwege, A.M. Hellwege (Eds.), Elastic, Piezoelectric, Pyroelectric, Piezooptic, Electrooptic Constants, and Nonlinear Dielectric Susceptibilities of Crystals, Vol. III/11 of Landolt-Bornstein, New Series, Springer-Verlag, New York, 1979, p. 245.
[14] W.H. Press, S.A. Teukolsky, W.T. Vetterling, B.P. Flannery, Numerical Recipes in FORTRAN: The Art of Scientific Computing, 2nd edition, Cambridge University Press, New York, 1992.
[15] D.C. Hurley, V.K. Tewary, A.J. Richards, Meas. Sci. Technol. 12 (2001) 1486.
[16] V.K. Tewary, J. Acoust. Soc. Am. 112 (2002) 925.
[17] W. Pang, A.G. Every, J.D. Comins, P.R. Stoddart, X. Zhang, J. Appl. Phys. 86 (1999) 311.
[18] A.J. Perry, Thin Solid Films 170 (1989) 63.
[19] R.Y. Fillit, A.J. Perry, Surf. Coat. Technol. 36 (1988) 647.
[20] J.O. Kim, J.D. Achenbach, Thin Solid Films 214 (1992) 25.
[21] W.J. Meng, G.L. Eesley, Thin Solid Films 271 (1995) 108.
[22] V.K. Tewary, Wave Motion 40 (2004) 399.
[23] D. Rafaja, V. Valvoda, R. Kuzel, A.J. Perry, J.R. Teglio, Surf. Coat. Technol. 86–87 (1996) 302.
[24] A.J. Perry, D.E. Geist, Surf. Coat. Technol. 94–95 (1997) 309.
[25] G. Wedler, J. Walz, T. Hesjedal, E. Chilla, R. Koch, Phys. Rev. Lett. 80 (1998) 2382.